Plasticizer effect on the dynamics of polyvinylchloride studied by dielectric spectroscopy and quasielastic neutron scattering

Reiner Zorn,[a] Michael Monkenbusch, and Dieter Richter
Forschungszentrum Jülich, IFF, D-52425 Jülich, Germany

Angel Alegría and Juan Colmenero
Departamento de Física de Materiales, Universidad del País Vasco, Apartado 1072, E-20080 San Sebastián, Spain

Bela Farago
Institut Laue-Langevin, B.P. 156X, F-38042 Grenoble, France

(Received 8 June 2006; accepted 31 August 2006; published online 20 October 2006)

We have studied the influence of plasticization on the microscopic dynamics of a glass-forming polymer. For this purpose we studied polyvinylchloride (PVC) with and without the commercially used plasticizer dioctylphthalate (DOP). We used dielectric spectroscopy and inelastic neutron scattering employing the neutron spin echo (NSE) technique. For both kinds of spectra the α relaxation could be consistently described by a model involving a distribution of individual relaxations of the Kohlrausch type. In contrast to earlier studies it turned out that an asymmetric distribution is necessary to fit the data at the lower temperatures investigated here. The shape parameters of the distribution (width, skewness) for PVC and PVC/DOP turned out to coincide when the characteristic relaxation times were the same. This means that the plasticizer only induces a remapping of the temperature dependence of the α relaxation. Comparison of NSE spectra $S(Q,t)/S(Q)$ at different scattering vectors Q gave the result that the slowing down at the structure factor peak $Q_{\max}$ is surprisingly small for PVC while it is in the normal range for PVC/DOP.
 [DOI: 10.1063/1.2357738]

I. INTRODUCTION

Many polymeric materials in practical use contain plasticizers (low molecular weight additives) to tailor their physical properties to particular technical needs. The main effect of the plasticizer consists in the reduction of the glass transition temperature T_g (plasticization effect). However, below T_g the plasticized polymers are often found to be more brittle than the pure polymer. This effect is usually referred to as antiplasticization. In the case of semicrystalline polymers, plasticization can also affect polymer crystallinity. One of the polymer/plasticizer systems more widely investigated is the system polyvinylchloride (PVC) and bis(2-ethyhexyl)phtalate [dioctylphtalate (DOP)]. The currently accepted structural point of view for this system is that plasticization does not affect significantly PVC crystallinity, even for DOP content as high as 50 wt %.[1,2] However, it has very recently been shown that PVC recovered from concentrated solution in DOP exhibits a higher ordered state than that obtained from solutions in other solvents. This would suggest that DOP could, in fact, have some effect on the PVC crystallinity.

The dielectric relaxation of PVC presents some peculiarities when compared with other polymers. Since very early works[3] the experiments showed that the dielectric α relaxation of PVC is unusually broad near T_g and narrows rapidly with increasing temperature, approaching the usual polymer behavior. In a previous paper[4] some of us investigated the relationship between structure and dynamics of PVC by combining neutron scattering and dielectric spectroscopy. In this way it was shown that the somehow anomalous dynamical behavior of PVC can be well accounted for by the existence of a heterogeneous structure. Through density modulations it causes a distribution of glass transition temperatures. This causes the (intrinsically broad) α relaxation to be additionally broadened by a distribution of characteristic times. The density modulations were found to be essentially temperature independent below 430 K and were associated with small microcrystalline nodules with a size of about 3 nm, the degree of crystallinity being about 4%.

Here we have used the same experimental approach to characterize the dynamics of plasticized PVC. Taking advantage of the high sensitivity of the polymer segmental dynamics to the structural heterogeneities we have investigated in very detail the effects of the plasticizer on the characteristics of the PVC crystallites.

In the present paper we have investigated the dynamics of both neat PVC and PVC plasticized with 9 wt % DOP. By combining dielectric relaxation spectroscopy and neutron spin echo techniques we covered a broad frequency/temperature range and we have accessed the microscopic structural relaxation. In the present study we have also extended the previous dielectric relaxation investigations on the segmental dynamics of PVC to lower temperatures by applying special sample conditioning procedures. The sample

[a]Author to whom correspondence should be addressed. Electronic mail: r.zorn@fz-juelich.de

preparation for the dielectric experiments was chosen to avoid any thermal degradation, which favors the ionic conductivity and consequently produces a significant increase of the dielectric loss at low frequencies above the glass transition temperature. Such a contribution to the dielectric loss would preclude a reliable analysis of the dipolar dielectric relaxation signal in the vicinity of the glass transition temperature range.

The paper is organized as follows: In Sec. II the sample preparation and the experimental techniques are described and typical experimental results of both nonplasticized and plasticized PVC as determined from dielectric relaxation are presented. Thereafter, in Sec. III the way of analysis is described. The results of this analysis are presented and compared in Sec. IV. Finally, in Sec. V the main results obtained are summarized.

II. EXPERIMENT

A. Samples

Commercial PVC and DOP samples were used for the dielectric experiments. For the neutron scattering experiments addressing the coherent scattering we used fully deuterated polymer and plasticizer. The deuterated polymer samples were synthesized by the group of Professor C. Mijangos (ICTP, CSIC, Madrid, Spain). Further details on the polymerization procedure can be found elsewhere. The characteristics of the deuterated polymer were already reported in Ref. 4. Deuterated DOP was purchased from CDN-Isotopes, Pointe-Claire, Canada. The deuteration level of DOP was 98.8% and that of the polymer was higher than 95%. The plasticized polymers were prepared by dissolving together DOP and PVC in tetrahydrofurane and drying the solution in a vacuum oven at 80 °C to produce films of about 0.1 mm thickness. The DOP content of the PVC/DOP samples used in this study was 9 wt %. The reference nonplasticized polymer samples were generated following the same solvent-casting procedure. The obtained samples were characterized by differential scanning calorimetry (Perkin Elmer DSC-4). The resulting glass temperatures were 358 K for PVC and 335 K for PVC/DOP. So the plasticized polymer shows a decrease of T_g as expected according to the DOP content.

B. Broadband dielectric spectroscopy

Dielectric measurements were performed in the frequency domain from 10^{-2} to 10^{9} Hz with a Novocontrol system by means of two different equipments. A Solartron-Schlumberger gain/phase analyzer SI1260 supplemented with a broadband dielectric converter allowed the dielectric relaxation to be measured in the range of 10^{-2}–10^{7} Hz. For higher frequencies (10^{6}–10^{9} Hz), a Hewlett-Packard impedance analyzer HP4191A based on the principle of a reflectometer was used. The error in the determination of the loss tangent of the dielectric constant was around 10^{-4} for the first setup and 10^{-2} for the second one. Superposition of the spectra at the same temperature was possible by means of the common decade of both equipments and small corrections were motivated by the uncertainties in the determination of the sample thickness. Sample holders, that act as electrodes, were parallel plate capacitors of 20 mm diameter for the low frequency setup and 5 mm diameter for the high frequency one. The thickness of the samples was 0.1 mm.

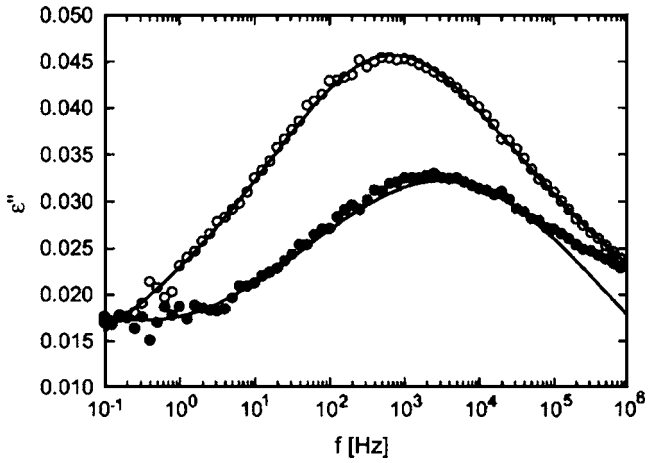

FIG. 1. Fits of the loss part of the dielectric function in the β relaxation regime of PVC at $T=260$ K (○) and PVC/DOP at $T=260$ K (●). The lines show fits with a sum of (11) and (12).

Measurements were made under isothermal conditions, each 5 K covering the temperature range relevant for the α and β relaxations of PVC with a temperature stability better than 0.1 K. We limited the temperature range investigated by dielectric spectroscopy to temperatures below 400 K since already at this temperature significant DOP loss was detected during the experimental acquisition time, likely favored by the fact that the sample capacitor was immersed in the nitrogen jet flow used by the temperature control system. As it will be depicted below the temperature range covered is wide enough to allow a complete comparison between the relaxation dynamics of nonplasticized PVC and plasticized PVC.

Figures 1 and 2 show typical dielectric spectra in the low and high temperature ranges. At low temperatures the extremely broad β relaxation is visible which extends over the whole frequency range. At higher temperatures the spectra consist of three components, in the order of ascending frequency: a conductivity tail at lowest frequencies, the α relaxation, and the β relaxation overlapped by the high frequency tail of the α relaxation. Figure 2 shows that the errors of the data increase strongly above 100 MHz. The reason for this is a resonance of the electrical circuit just above 1 GHz which cannot be fully compensated. We stress that these errors do not significantly affect the main results on the α relaxation whose maximum frequency is always below 10 MHz for the temperatures studied.

C. Neutron spin echo spectroscopy

The experimental result of neutron spin echo (NSE) is the normalized intermediate scattering function $S(Q,t)/S(Q)$. Because the samples used here were completely deuterated the observed scattering is mainly coherent from two-particle correlations. This is even more pronounced because NSE registers coherent scattering with three times the weight of spin-incoherent scattering. Therefore, $S(Q,t)/S(Q)$ represents the density-density autocorrelation function:

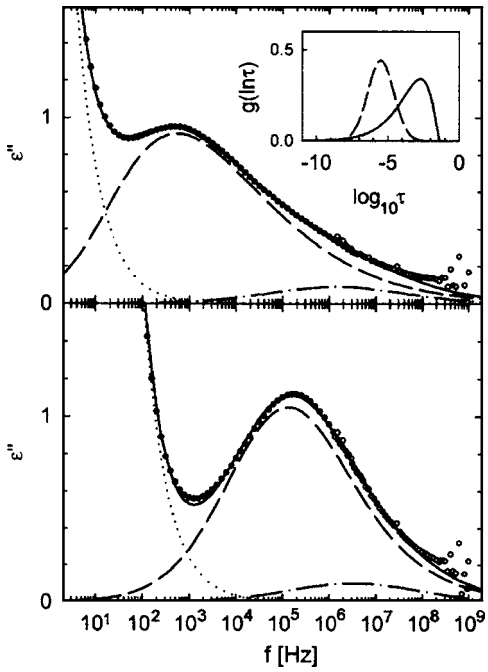

FIG. 2. Examples of fits of the α relaxation loss peak for (pure) PVC at $T=370$ K (upper graph) and $T=390$ K (lower graph). The filled symbols are from the low frequency measurements ($f<5$MHz), while the empty symbols result from the high frequency setup ($f=1.5$ MHz–1 GHz). The continuous curve denotes the total fitted ϵ''. The other curves show the following components: (---) α relaxation, Eq. (7); (--) β relaxation, Eq. (11); and (···) conductivity, Eq. (19). The inset in the upper graph shows the distributions used for fitting the α relaxation for $T=370$ K (—) and $T=390$ K (---).

$$\frac{S(Q,t)}{S(Q)}=\frac{\langle\Delta\rho_Q(0)\Delta\rho_Q(t)\rangle}{\langle\Delta\rho_Q(0)\Delta\rho_Q(0)\rangle}. \tag{1}$$

Here, $\Delta\rho_Q(t)$ indicates the Fourier components of the density fluctuations and Q is the scattering vector determined by the wavelength λ of the scattered neutrons and the scattering angle 2θ:

$$Q=\frac{4\pi}{\lambda}\sin\theta. \tag{2}$$

Two different experimental setups have been used.

1. IN11A at ILL Grenoble

This is a standard NSE with a single secondary arm. So during one run $S(Q,t)/S(Q)$ is only recorded for one Q value. The incident wavelength was chosen as 4.3 Å for $Q=1.2$ Å^{-1} and 4.7 Å for $Q=1.5$ Å^{-1}, yielding time ranges of 0.0035–2.9 ns and 0.0030–1.8 ns, respectively. It has to be kept in mind that the incident wavelength selection is $\Delta\lambda/\lambda=0.2$ here. This means that the uncertainty of Q is, e.g., 1.2 ± 0.12 Å^{-1} (error margins defined as the points where the intensity falls off to half its peak value).

2. NSE at FZ Jülich

The Jülich NSE (see table of contents graphic) is a modified standard setup with a two-dimensional multidetector at the end of the secondary arm. At high angles, as they are necessary to achieve the high Q values to be studied here, the multidetector is rather used to improve statistics than to obtain several Q values. Due to an elaborate arrangement of correction coils very high t values in $S(Q,t)/S(Q)$ can be obtained. For an incident wavelength of 7 Å (used for $Q=1.17$ Å^{-1}) the t range was 0.063–14.7 ns, and for 6 Å ($Q=1.4$ Å^{-1}) $t=0.040$–9.3 ns. On this instrument the wavelength is selected to 10%, yielding a higher accuracy of Q, e.g., 1.17 ± 0.06 Å^{-1}.

III. DATA ANALYSIS

A. Distribution model for the α relaxation in PVC

The relaxation spectra of glass-forming systems usually contain at least two separable contributions, the α and the β relaxation. (The latter will be introduced in the following subsection.) The α relaxation shows a strong temperature dependence and its slowing down upon cooling defines the kinetic glass transition. In the α relaxation regime the decay of correlation functions in time domain can be described empirically by the stretched-exponential or Kohlrausch law:

$$\Phi(t)=\exp(-(t/\tau_K)^\beta), \tag{3}$$

where the exponent is in the range $\beta=0$–1.

The basic idea of the model[4] used to fit neutron scattering and dielectric data in PVC is that of a *distribution of relaxations* which are individually of Kohlrausch type. Here, the Kohlrausch function with $\beta<1$ reflects the *intrinsic* broadening of the α relaxation while the distribution $g(\ln\tau_K)$ results from the *heterogeneous structure*.[4] This leads to the expression

$$\Phi(t)=\int_{\tau_K=0}^{\infty} d\ln\tau_K g(\ln\tau_K)\exp(-(t/\tau_K)^\beta). \tag{4}$$

It is assumed that the stretching parameter β is not distributed such that the shape of $\Phi(t)$ is solely determined by the distribution function $g(\ln\tau_K)$. A function reflecting the specific asymmetry of the data which reduces to the more common log-normal distribution in the case of vanishing asymmetry was chosen—namely, a rescaled gamma distribution, Eqs. (A1) and (A2).

Because NSE experiments provide a result in time domain, expression (4) can be used directly to fit the data. It is only necessary to add a prefactor (similar to a Debye-Waller factor) to account for the reduction of the signal due to motions which are outside the time window of NSE:

$$S(Q,t)/S(Q)=f_Q\Phi(t). \tag{5}$$

In order to keep the number of fit parameters small, an exponential decay of f_Q with temperature was assumed:

$$f_Q=A\exp(-DT). \tag{6}$$

This expression is strictly valid, e.g., in classical approximation for harmonic vibrations as a source of the fast dynamics. But here it should be understood as an empirical description only. It should be pointed out that fits without this assumption vary only within the statistical error of the parameters.

The dielectric experiments were carried out in the frequency domain. Therefore, in principle the Fourier transform of (4) should be used to fit the data. But since numerical

studies[5,6] have shown that this Fourier transform can be substituted by the Havriliak-Negami function with sufficient accuracy we used

$$\epsilon''_\alpha(\omega) = -\Delta\epsilon_\alpha \Im\left(\int_{\tau_K=0}^{\infty} d\ln\tau_K g(\ln\tau_K)\frac{1}{(1+(i\omega\tau_{HN})^\alpha)^\gamma}\right) \tag{7}$$

[where $\Im(\cdots)$ indicates the imaginary part] with the following system of equations relating the Havriliak-Negami parameter α, γ, and τ_{HN} to the Kohlrausch parameters β and τ_K:

$$\alpha\gamma = \beta^{1.23}, \tag{8}$$

$$\log_{10}(\tau_{HN}/\tau_K) = 2.6(1-\beta)^{0.5}\exp(-3\beta), \tag{9}$$

$$\gamma = 1 - 0.8121(1-\alpha)^{0.387}. \tag{10}$$

The maximal absolute deviation of this approximation from the true Fourier transform of the Kohlrausch function is 4.3% of the peak value, therefore in the order of the experimental error of the ϵ'' data. Also we prefer to use this expression to be completely consistent with the earlier data evaluation in Ref. 4.

B. β relaxation

In addition to the contribution of the α relaxation the dielectric spectra clearly show the presence of a β relaxation which overlaps with the α relaxation at high temperature. The β relaxation was modeled using a log-normal distribution for the loss part:

$$\epsilon''_\beta(\omega) = \sqrt{\frac{\pi}{8}}\frac{\Delta\epsilon_\beta}{W_\beta \ln 10}\exp\left(-\frac{(\log_{10}(\omega\tau_\beta))^2}{2W_\beta^2}\right). \tag{11}$$

From the picture of the β relaxation as a superposition of exponential relaxations with a log-normal distribution of relaxation times a distribution *integral* similar to (7) with $\beta = 1$ would be more correct. But this approximation is justified because our primary interest here is the α relaxation and also the width W_β turns out to be large compared to that of a Debye function (0.557).

Above a certain temperature the dielectric loss curves develop an upturn at low frequencies, which obviously cannot be represented by a monomodal distribution as (11). Therefore, it was necessary to include a fractal contribution in the fit:

$$\epsilon''_{fract}(\omega) = a\omega^{-x}. \tag{12}$$

On the other hand the temperatures are still so low that an explanation as for the formally identical contribution (19) to the α relaxation (see below) by conductivity/interfacial effects cannot hold, rather the empirical formula (12) should be the high frequency wing of the α relaxation. The exponent x is also much smaller than for conductivity. It was kept constant for each sample being $x=0.128$ for PVC and 0.113 for PVC/DOP. x is also much smaller than the asymptotic value $\alpha\gamma$ expected from the Havriliak-Negami description done in Sec. III C. This can be understood from the fact that the α relaxation peak is too close to allow the asymptotic representation as a power law. On the other hand an exponent as low as 0.1–0.15 would be compatible with the α relaxation having an "excess wing" where $\epsilon''(\omega)$ departs from the Havriliak-Negami asymptotics observed in some glass formers, e.g., glycerol.[7] The prefactor a was fitted individually for each temperature, resulting in values which strongly increase with temperature which is the expected behavior if the α relaxation peak approaches the frequency window.

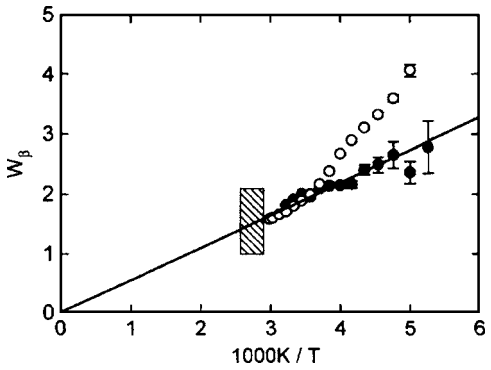

FIG. 3. Width of the β relaxation loss peak obtained from fits of (11)+(19) as shown in Fig. 1 for PVC (○) and PVC/DOP (●). The line represents relation (13) used for extrapolation. The shaded area denotes the temperature range to which the results have been extrapolated.

As Fig. 1 shows, the main effect of plasticization on the β relaxation is a reduction of its strength, wherein the area under the loss peak is smaller. This has been reported earlier[8] and will not be discussed here. Nevertheless, in order to obtain stable parameters for the α relaxation it is necessary to describe the β relaxation empirically and extrapolate it to the region where the α and β peaks overlap in the dielectric spectra.

For this purpose the dielectric spectra at low temperatures (200–340 K for PVC and 190–310 K for PVC/DOP) were fitted by a sum of (11) and (12). At these temperatures only the β peak and—if anything at all—the high frequency wing of the α relaxation are visible. Figure 1 shows some representative fits in this region.

In order to predict the β relaxation at higher temperatures three parameters have to be extrapolated: W_β, τ_β, and $\Delta\epsilon_\beta$. Especially for low temperatures, W_β is different for plasticized and neat PVC (Fig. 3). Nevertheless, in the high temperature limit this parameter seems not to depend on the plasticizer content. For both samples it shows an inverse proportionality with the same factor for PVC and PVC/DOP to temperature, namely,

$$W_\beta = 546 \pm 1\ \mathrm{K}/T. \tag{13}$$

With respect to the (logarithmic) average relaxation time τ_β both samples show a clear difference. The β relaxation is *faster* in the plasticized material, similar to the α relaxation. For both samples the temperature dependence is Arrhenius type (Fig. 4) at higher temperatures:

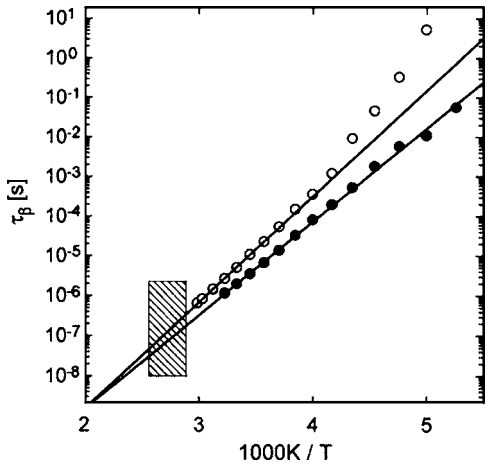

FIG. 4. Center of the β relaxation loss peak obtained from fits of (11)+(19) as shown in Fig. 1 for PVC (○) and PVC/DOP (●). The lines represent fits with the Arrhenius expression (14). The shaded area denotes the temperature range to which the results have been extrapolated.

$$\tau_\beta = \tau_\beta^0 \exp(E_A/k_B T), \tag{14}$$

with $\tau_\beta^0 = 6.9 \pm 0.9 \times 10^{-15}$ s, $E_A = 6140 \pm 40$ K k_B for PVC, and $\tau_\beta^0 = 3.0 \pm 0.5 \times 10^{-14}$ s, $E_A = 5400 \pm 40$ K k_B for PVC/DOP. If one interprets W_β in (13) as resulting from a distribution of energy barriers it would correspond to about 10% width.

We have to note that in the case of pure PVC there is a noticeable curvature in the activation plot (Fig. 4), leading to a significant deviation for $T < 250$ K. Also there is a departure from the $1/T$ increase of the width W_β below 280 K (Fig. 3). Furthermore, the prefactor τ_β^0 for PVC is extremely small. These findings cast some doubt on the usual energy barrier interpretation. A possible explanation would be the picture of "two types" of β relaxation in PVC.[9] In this context the acceleration of the β relaxation by the plasticizer could also be explained as a selective suppression of the slower type of β relaxation.

Concerning the third parameter to be extrapolated it turned out to be easier to do this on the β peak height $\epsilon''_{\max} = \sqrt{\pi/8}\Delta\epsilon_\beta / W_\beta \ln 10$ than on the relaxation strength $\Delta\epsilon_\beta$ itself. A fit was possible using an exponential temperature dependence:[10]

$$\epsilon''_{\max} = B \exp(CT), \tag{15}$$

with $B = 4.76 \pm 0.08 \times 10^{-3}$ and $C = 8.36 \pm 0.05 \times 10^{-3}$ K^{-1} for PVC and $B = 2.57 \pm 0.04 \times 10^{-3}$ and $C = 9.20 \pm 0.06 \times 10^{-3}$ K^{-1} for PVC/DOP.

We note that the uncertainties of this empirical description do not invalidate its use in the following to separate out the α contribution. As can be seen from Figs. 3 and 4 the temperature region to where the β relaxation is extrapolated is very close to the range where the parameters are derived from. Therefore, alternative extrapolations (e.g., a non-Arrhenius fit for τ_β in neat PVC) are not expected to give much different results. A more problematic situation would be a discontinuous change of the β relaxation parameters at T_g. Around T_g the β and α relaxations are already overlapping so that no individual fit of the β relaxation is possible. This is due to the peculiarity that the α relaxation in PVC and PVC/DOP is very broad. In consequence, there is no way to confirm nor to rule out a β parameter discontinuity. But since the β relaxation only has about 10% of the strength of the α relaxation (Fig. 2) it can be expected that a misinterpretation of a part of the β relaxation as included in the α relaxation distribution does not have a big impact on the α relaxation parameters determined below.

C. α relaxation: Dielectric spectroscopy

The dielectric loss data at higher temperatures were fitted with a sum of α relaxation (7), β relaxation (11), and conductivity (19) contributions. The parameters of the β relaxation were fixed according to the extrapolation described in the preceding section. At the current stage of the investigation we do not attempt a more involved combination method as, e.g., convolution.[11]

From earlier experience on PVC (Ref. 4) the Kohlrausch exponent was fixed to $\beta = 0.5$, resulting in Havriliak-Negami parameters $\alpha = 0.779$ and $\beta = 0.547$ in Eq. (7).

The Havriliak-Negami times were assumed to be distributed according to the rescaled gamma function from (A1) and (A2):

$$\begin{aligned} g(\ln \tau_{HN}) &= \frac{b/\ln 10}{\Gamma(p)} \left(b \log_{10} \frac{\tau_{\max}}{\tau_{HN}} \right)^{p-1} \\ &\quad \times \exp\left(- b \log_{10} \frac{\tau_{\max}}{\tau_{HN}} \right) \\ &= \frac{b^p}{\ln 10 \Gamma(p)} \left(\log_{10} \frac{\tau_{\max}}{\tau_{HN}} \right)^{p-1} \left(\frac{\tau_{\max}}{\tau_{HN}} \right)^{-b/\ln 10}. \end{aligned} \tag{16}$$

For the purpose of easier comparison the maximal Havriliak-Negami time $\tau_{\max}$ appearing as a parameter in (16) is converted to the average logarithmic Kohlrausch time by relations (A4) and (9) with $\beta = 1/2$:

$$\begin{aligned} \langle \log_{10} \tau_K \rangle &= \langle \log_{10} \tau_{HN} \rangle + 0.387 \\ &= \langle \log_{10} \tau_{\max} \rangle - p/b + 0.387. \end{aligned} \tag{17}$$

Also instead of b in Eq (16) the logarithmic width from (A6) was used:

$$W = \sqrt{p}/b. \tag{18}$$

In all dielectric spectra at higher temperatures and low frequencies a contribution could be found which is related to conductivity and interfacial effects. As in the case of the β relaxation (see above) but a with a different reason this was modeled by a "fractal" contribution:

$$\epsilon''_{\text{cond}}(\omega) = a\omega^{-x}, \tag{19}$$

with $x \lesssim 1$. In order to reduce the number of free parameters further, the exponent x in (19) was fixed for each sample. For that purpose the conductivity slope was fitted by a power law in the range $\epsilon'' = 2-10$, which appears linear in a double logarithmic plot. The resulting x was 0.845 in the case of PVC and 0.747 for PVC/DOP.

In summary, the five free parameters fitted at each temperature were the α relaxation strength $\Delta\epsilon_\alpha$, the average

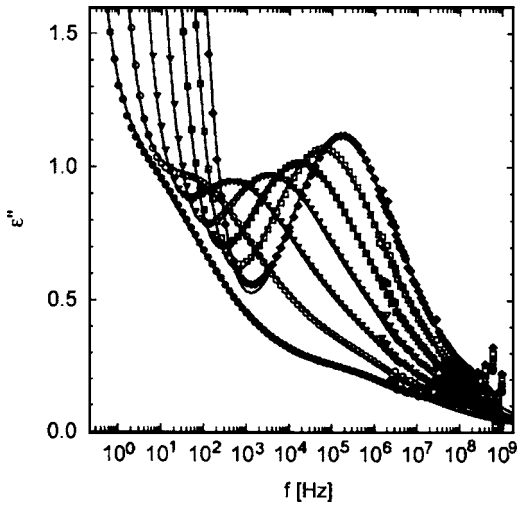

FIG. 5. Fits of the dielectric loss $\epsilon''(f)$ of (pure) PVC for all available temperatures: (●) 360 K, (○) 365 K, (▼) 370 K, (▽) 375 K, (■) 380 K, (□) 385 K, and (♦) 390 K. The continuous curves show the fits with a sum of (7), (11), and (19).

logarithmic Kohlrausch time $\langle \log_{10} \tau_K \rangle$, the width of the distribution W, p as a measure of its skewness, and the conductivity strength a of expression (19).

Figure 2 shows examples of the fits for PVC without DOP at temperatures near the lower and the higher limits of the possible temperature range. For temperatures <360 K (345 K for PVC/DOP) the fit was impossible because the α relaxation loss peak was swamped by the conductivity slope. Higher temperatures than 390 K were not studied to avoid degradation of the polymer. The inset in Fig. 2 shows the distribution functions. It can be clearly seen that there is a tendency to a more symmetric distribution function when the temperature is raised.

Figures 5 and 6 show the fits for all available data. It can be seen that the fit represents the α relaxation peak shape well. Deviations are visible for high temperatures in the minimum between the conductivity slope and the peak and

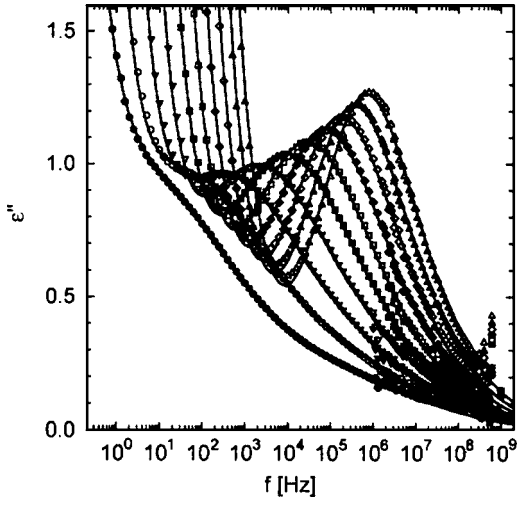

FIG. 6. Fits of the dielectric loss $\epsilon''(f)$ of PVC/DOP for all available temperatures: (●) 345 K, (○) 350 K, (▼) 355 K, (▽) 360 K, (■) 365 K, (□) 370 K, (♦) 375 K, (◇) 380 K, (▲) 385 K, and (△) 390 K. The continuous curves show the fits with a sum of (7), (11), and (19).

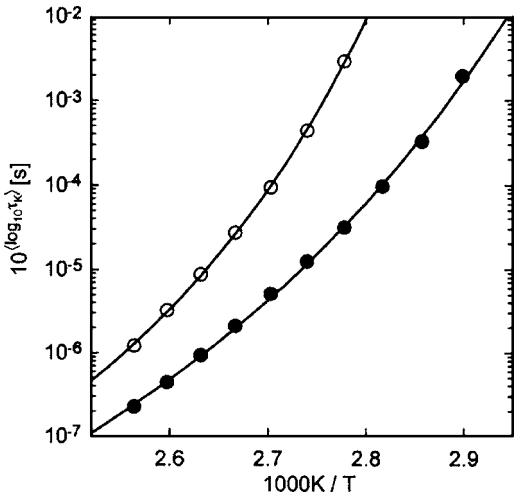

FIG. 7. Average logarithmic Kohlrausch times of the α relaxation. The empty symbols represent data from PVC, while the filled ones PVC/DOP. The curves are fits with the VFT expression (20).

(especially for pure PVC) at the highest frequencies $f > 50$ MHz. The former can be removed if one fits the conductivity exponent x as a temperature dependent parameter. But this would lead to an instability of the fit at low temperatures. The high frequency deviations may be due to a systematic error of the high frequency setup which becomes visible because of the low absolute values $\epsilon'' < 0.1$. On the other hand the already mentioned "double" β relaxation of PVC (Ref. 9) may be the origin. In any case this feature is separated by some decades in frequency from the α relaxation so that it has negligible influence on the α relaxation parameters to be discussed here.

Figure 7 shows the average logarithmic Kohlrausch time (17) in the usual Arrhenius representation, i.e., versus the reciprocal temperature. The non-Arrhenius character which is expected for an amorphous material can be clearly seen from the curvature. The curves show fits with the Vogel-Fulcher-Tamman (VFT) relation,

$$10^{\langle \log_{10} \tau_K \rangle} = \tau_\alpha^0 \exp\left(\frac{B}{T - T_0}\right), \tag{20}$$

with the parameters shown in Table I. The fits describe the

TABLE I. Parameters of the dielectrically observed α relaxation for PVC and PVC/DOP. The VFT fit by Eq. (20) has been done on a logarithmic ordinate. Therefore $\log_{10}(\tau_\alpha^0/\mathrm{s})$ is the actual fit parameter. Because of its large error estimate linear error propagation does not make sense and the error estimate for τ_α^0 is omitted. a_W and a_γ are the coefficients of the dependence of the distribution width and skewness, respectively, on the characteristic time as defined in Eqs. (21) and (22).

	PVC	PVC/DOP
B (K)	1211±16	1770±32
T_0 (K)	305±4	270±8
τ_α^0 (s)	9×10^{-13}	1×10^{-13}
$\log_{10}(\tau_\alpha^0/\mathrm{s})$	−12.07±0.5	−13.02±0.7
a_W	0.319±0.014	0.307±0.009
$\log_{10}(\tau_W^{\mathrm{lim}}/\mathrm{s})$	−8.66±0.19	−8.60±0.11
a_γ	0.360±0.009	
$\log_{10}(\tau_\gamma^{\mathrm{lim}}/\mathrm{s})$	−5.79±0.04	

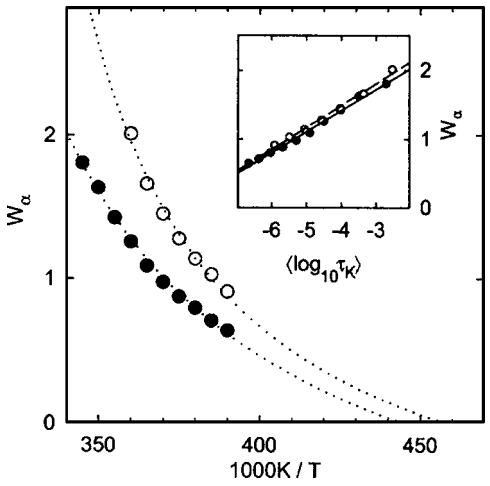

FIG. 8. Width of the distribution of Kohlrausch times of the α relaxation. The inset shows the linear relation between the width and the average logarithmic Kohlrausch time. The empty symbols represent data from PVC, while the filled ones PVC/DOP. The dotted lines in the main plot are extrapolations to high temperatures using the linear relation (21) and the VFT expression (20).

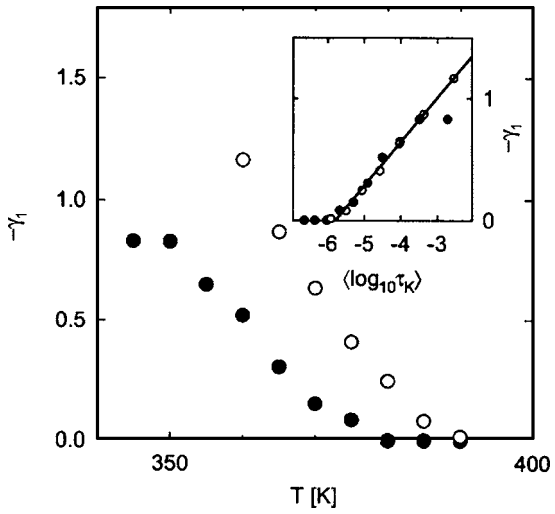

FIG. 9. Skewness of the distribution of Kohlrausch times of the α relaxation. The empty symbols represent data from PVC, while the filled ones PVC/DOP. The inset shows the linear relation between the skewness and the average logarithmic Kohlrausch time.

data within ±5% for PVC and ±20% for PVC/DOP. On the other hand the parameters (especially τ_α^0) are not well defined because of the small temperature range. But because we use this fit primarily for extrapolation into the region where the NSE experiments were done, this description is sufficient.

The width of the distribution of Kohlrausch times W_α, displayed in Fig. 8, clearly behaves different from the width W_β related to the β relaxation (Fig. 3). The dependence on $1/T$ is nonlinear and also extrapolates to $W_\alpha=0$ at a finite temperature. It is very similar to the temperature dependence of the average logarithmic Kohlrausch time. Indeed, as the inset in Fig. 8 shows, there is a linear relation,

$$W_\alpha = a_W(\langle \log_{10} \tau_K \rangle - \log_{10} \tau_W^{\lim}), \tag{21}$$

between the width and the average logarithmic Kohlrausch time. The coefficients of this relation (Table I) are indistinguishable within error limits. The extrapolation indicates that the distribution collapses to a single value when the average Kohlrausch time reaches $\tau_W^{\lim}=2.5\pm0.5$ ns which corresponds to temperatures of 458 and 445 K for PVC and PVC/DOP, respectively. This means that at a temperature of 100–110 K above T_g the *dynamic* heterogeneity vanishes and the α relaxation can be described by a single Kohlrausch function.

As Fig. 9 shows, the skewness of the distribution behaves very similar as the width. One can again find a linear relation,

$$\gamma_1 = -a_\gamma(\langle \log_{10} \tau_K \rangle - \log_{10} \tau_\gamma^{\lim}), \tag{22}$$

with the average logarithmic Kohlrausch time. Again the relation is the same for PVC and PVC/DOP. But the limiting average Kohlrausch time is much longer than in the former case: $\tau_\gamma^{\lim}=1.62\pm0.15$ μs. Thus the distribution loses its asymmetry at 389 or 377 K for PVC and PVC/DOP, respectively. This is about 70 K below the temperature where the distribution collapses completely.

Finally, Fig. 10 shows the strength of the α relaxation, i.e., the prefactor $\Delta\epsilon_\alpha$ in (7). There is only a small variation (less than 6%) of $\Delta\epsilon_\alpha$ between the two specimens and over the temperature range investigated. Nevertheless, a faint maximum can be observed for both samples. As the inset shows this maximum occurs when the average logarithmic Kohlrausch time reaches a value about 0.03–0.1 ms for both PVC and PVC/DOP. It has to be noted that this result relies on the fits of the two lowest temperatures for both samples—360 and 365 K for PVC and 340 and 245 K for PVC/DOP. At these temperatures the α relaxation time is very large, so that the peak is overlapped by the conductivity contribution. Therefore, the separation of the conductivity is more difficult so that the parameter $\Delta\epsilon_\alpha$ is not as reliable as at higher temperatures.

D. α relaxation: Neutron spin echo spectroscopy

Figures 11 and 12 show NSE spectra of undoped PVC close to the first maximum and in the first minimum of the structure factor $S(Q)$ of PVC.

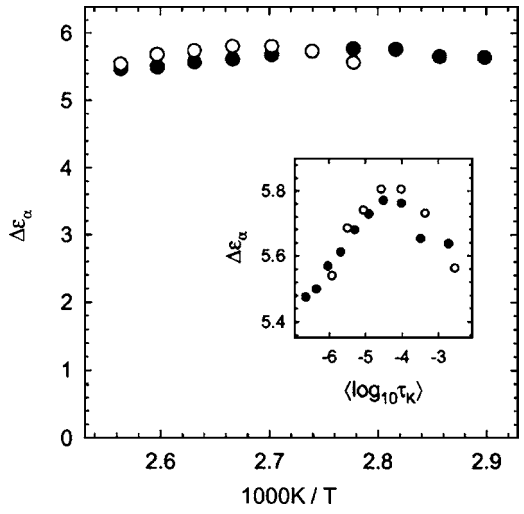

FIG. 10. Strength $\Delta\epsilon_\alpha$ of the α relaxation. The empty symbols represent data from PVC, while the filled ones PVC/DOP. The inset shows that the values for PVC and PVC/DOP are approximately equal at same average logarithmic Kohlrausch times.

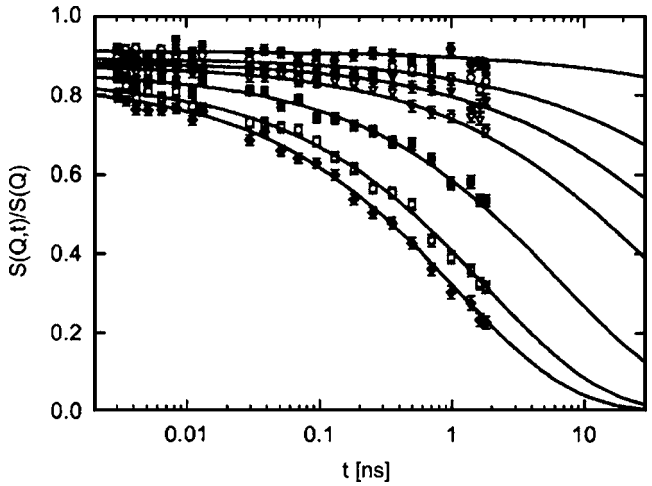

FIG. 11. Neutron spin echo data (IN11A, ILL Grenoble) of the coherent intermediate scattering function $S(Q,t)/S(Q)$ of PVC without DOP at $Q=1.2$ Å^{-1} at temperatures of (●) 370 K, (○) 390 K, (▼) 400 K, (▽) 410 K, (■) 430 K, (□) 450 K, and (♦) 460 K. The continuous curves show the fits with the model described in the text.

It can be seen that the fit with the model (4) works very well with most parameters transferred from the fits of the dielectric data. Only A and D determining the Debye-Waller factor via (6) and the ratio of the central relaxation times,

$$\log_{10} R_{\mathrm{NSE/D}} = \langle \log_{10} \tau_{\mathrm{K}}^{\mathrm{NSE}} \rangle - \langle \log_{10} \tau_{\mathrm{K}}^{\mathrm{diel}} \rangle, \tag{23}$$

were fitted. All temperatures are described by a single parameter set for each Q value and sample (Table II). The fact that $A>1$ seems unphysical but the f_Q resulting from (6) is always smaller than 1. This only means that $-\ln f_Q(T)$ is not linear over the whole temperature range from 0 K and has a higher slope in the interval where the measurements were done than at lower temperatures.

The corresponding NSE data for PVC with 9% DOP are presented in Figs. 13 and 14. By neutron diffraction it has been verified that the position of the structure factor peak is unchanged by DOP plasticization.[12,13] Therefore, the Q values have the same "meaning" for both samples; 1.2 Å^{-1} represents the structure factor peak while 1.4 Å^{-1} is close to the first minimum in $S(Q)$. One can see that the model fit works equally well for the plasticized PVC. If one compares the spectra at identical temperatures (e.g., 390 K) it is visible directly from the data that the slowing down at the structure factor peak is more pronounced here than for pure PVC.

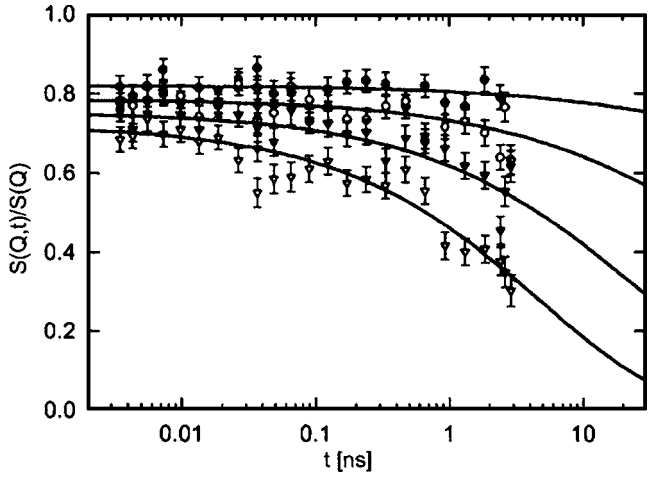

FIG. 12. Neutron spin echo data (IN11A, ILL Grenoble) of the coherent intermediate scattering function $S(Q,t)/S(Q)$ of PVC without DOP at $Q=1.5$ Å^{-1} at temperatures of (●) 370 K, (○) 390 K, (▼) 410 K, and (▽) 430 K. The continuous curves show the fits with the model described in the text.

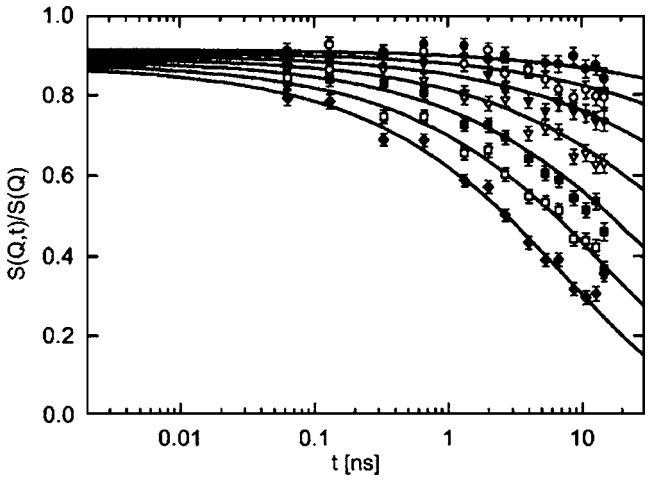

FIG. 13. Neutron spin echo data of the coherent intermediate scattering function $S(Q,t)/S(Q)$ of PVC with 9% DOP. Upper curves, left ordinate: IN11C, ILL Grenoble, $Q=1.2$ Å^{-1}. Lower curves, right ordinate: NSE Jülich, $Q=1.17$ Å^{-1}. Temperatures: (●) 360 K, (○) 370 K, (▼) 380 K, (▽) 390 K, (■) 400 K, (□) 410 K, and (♦) 420 K. The continuous curves show the fits with the model described in the text. The parameter D is coupled between both data sets, while all other parameters are fitted individually, especially allowing different characteristic times for the Grenoble and Jülich data.

IV. DISCUSSION

For the better understanding of the following discussion we first rephrase the heterogeneous structure model (HSM) of Ref. 4: Small-angle neutron scattering (SANS) experiments have shown that PVC in contrast to other polymers shows a heterogeneous structure on a length scale of some nanometers. Because different densities observed by SANS imply different glass transition temperatures, from this follows a distribution $h(T_0)$ of VFT temperatures in Eq. (20). Ideally, the heterogeneous structure and therefore $h(T_0)$ should be temperature independent. Because at a certain sample temperature different domains have different temperature distances $T-T_0$ to the VFT temperature, the VFT equation (20) produces a distribution of relaxation times, $g(\log_{10} \tau_{\mathrm{K}})$. The latter distribution is *always* temperature dependent because of the nonlinearity of the VFT relation. Especially, one expects the distribution $g(\log_{10} \tau_{\mathrm{K}})$ to collapse for high temperatures because the VFT relation flattens for large differences $T-T_0$.

With respect to the dielectric data on the α relaxation of undoped PVC we note that they agree with an earlier study using the HSM on similar samples of PVC (Ref. 4) in the overlapping temperature range of both studies: The position and width of the distribution $g(\log_{10} \tau_{\mathrm{K}})$ are identical. Also the extrapolated point where the width vanishes (here, 458 K) agrees with the value determined in Ref. 4, 464 K.

TABLE II. Parameters from the fits of the α relaxation in the NSE spectra. A and D determine the Debye-Waller factor via (6). $R_{NSE/D}$ is the ratio of the central relaxation times of NSE and dielectric spectra [Eq. (23)]. Together with the VFT parameters and width parameters in Table I it determines the NSE relaxation time distribution for all temperatures.

Sample	Q (Å^{-1})	A	D	$R_{NSE/D}$	τ_K^{NSE}(390 K) (ns)
PVC	1.2	1.8±0.2	$2.1\pm0.3\times10^{-3}$	0.529±0.013[a]	679±17
PVC	1.5	1.30±0.03	$0.97\pm0.06\times10^{-3}$	0.38±0.05[a]	490±70
PVC/DOP	1.2	1.20±0.10	$0.8\pm0.2\times10^{-3}$	0.70±0.04[b]	167±8
PVC/DOP	1.4	1.3±0.2	$1.3\pm0.5\times10^{-3}$	0.105±0.009[b]	25±2

[a]IN11A, Grenoble data.
[b]NSE, Jülich data.

Nevertheless, in the earlier study all fits were done with a symmetric distribution while here a skewed distribution was applied. But this is no contradiction because the former study covered a higher temperature range (380–430 K) where the skewness becomes negligible according to our results. This different temperature range is also the origin of the different VFT parameters here and in Ref. 4.

For the DOP plasticized PVC the picture is similar: Fig. 15 shows the distribution $h(T_0)$ of the regions calculated back from $g(\log_{10}\tau_K)$ according to the HSM. One can see that for high temperatures, 375–390 K, the curves coincide. This means that in the high temperature range the HSM is applicable with a temperature independent distribution of structures. The distribution $h(T_0)$ is slightly broader in the case of PVC/DOP, its full width at half maximum being 27 K as compared to 22 K for pure PVC. In the model picture this would mean that the plasticization enhances either the density modulation of the sample or the coupling of density and glass temperature—a question which cannot be answered without small-angle diffraction data on the plasticized samples.

At temperatures $\leqslant$370 K a noticeable skewness of the distribution $g(\ln\tau_K)$ develops (Fig. 9) and consequently the shape of $h(T_0)$ changes. It is interesting that for PVC/DOP this onset temperature is higher with respect to T_0 so that there is a larger temperature range in which skewed $g(\ln\tau_K)$ distributions are necessary to describe the data. Nevertheless, plotted against (logarithmic) average relaxation time (inset of Fig. 9) the onset lies at identical positions, namely, 1.6 μs for PVC and PVC/DOP. From this it can be concluded that the deviation from the model of invariant spatial heterogeneities happens at the same mobility of the sample and the different onset temperatures are only a consequence of the different VFT laws (20), PVC/DOP being the more fragile[14] material of both.

The difference in fragility together with the possibility to describe both samples with the same Kohlrausch β of 1/2 on the first glance seems to contradict the correlation between β and fragility found by a statistics of literature data.[15] But one has to note that the difference of fragilities is comparatively small in terms of the fragility measure used in Ref. 15: $m \equiv d\log_{10}\tau/d(T_g/T)|_{T=T_g}=129$ for PVC and 94 for PVC/DOP. Even within the material class of polymers Ref. 15 lists differences up to 40 in m for identical β values. The other question is whether the β-m relation of Ref. 15 also applies for the *intrinsic* β value determined here as 1/2 since it is derived using *apparent* β values from simple Kohlrausch fits which interpret the effect of a convolution [Eq. (4)] as a lowering of β.

We now turn to the comparison with the NSE data firstly

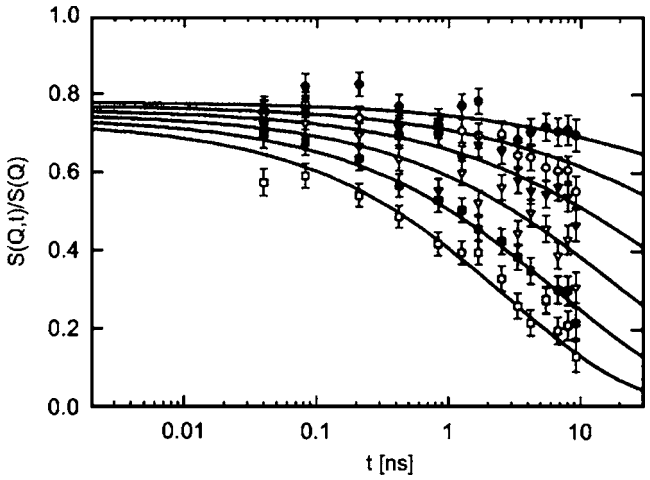

FIG. 14. Neutron spin echo data of the coherent intermediate scattering function $S(Q,t)/S(Q)$ of PVC with 9% DOP at Q=1.4 Å^{-1}. Data without error bars: IN11C, ILL Grenoble. Data with error bars: NSE Jülich. Temperatures: (●) 360 K, (○) 370 K, (▼) 380 K, (▽) 390 K, (■) 400 K, and (□) 410 K. The continuous curves show the fits with the model described in the text. Grenoble and Jülich data were fitted by *one* parameter set here.

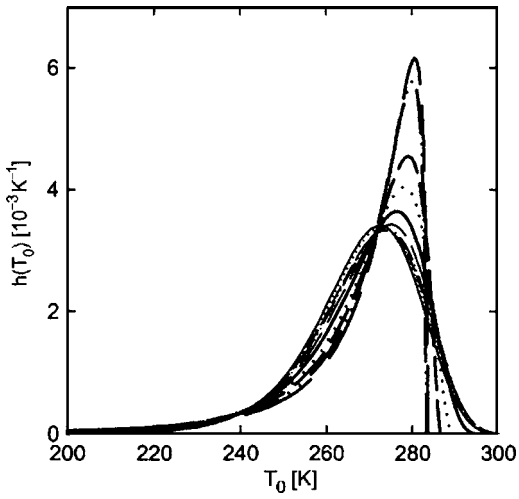

FIG. 15. Distribution $h(T_0)$ of VFT temperatures calculated according to the model in Ref. 4 for PVC/DOP. Temperatures (thin lines): (—) 390 K, (···–···) 385 K, (----) 380 K, (·–·–·) 375 K, and (– –) 370 K. Temperatures (thick lines): (—) 365 K, (·–·–·) 360 K, (----) 355 K, (-·-·-) 350 K, and (-··-··) 345 K.

noting that the skewness of $g(\ln \tau_K)$ is not very important there because those NSE spectra exhibiting a strong decay were taken in the respective high temperature ranges of PVC and PVC/DOP where γ_1 is negligible.

We have shown that for both PVC and PVC/DOP the data from NSE and dielectric spectroscopy can be reconciled by a simple model relying on two assumptions: (1) The relaxations observed by both methods arise from the same distribution $g(\ln \tau_K)$ of individual relaxation processes. (2) The individual process follows a Kohlrausch law $\exp(-(t/\tau)^\beta)$ with the same exponent β for both methods. This is what is expected from the assumption of dynamical heterogeneity. Nevertheless, the experiment only tells us that the combination (1)+(2) is true, i.e., that the shape of the averaged relaxation is identical for both methods. This could also be explained, e.g., by the α relaxation universality implied by mode coupling theory.[16] Nevertheless, this theory would have difficulties in explaining the drastic violation of the time-temperature superposition principle, the narrowing of relaxation peaks towards higher temperatures.

This fact is consistently explained here by the argument that an identical range ΔT_0 of VFT temperatures in different regions causes a larger spread $W^2=\langle \Delta \log_{10} \tau_K^2 \rangle$ of (logarithmic) relaxation times if the temperature is closer to the average T_0. This can be easily seen by taking the derivative of Eq. (20). As was pointed out before[4] the model also explains the anomalous low β value of PVC listed in the literature,[15] namely, 0.24. In addition it accounts for the seeming paradox that the (apparent) β value from quasielastic neutron scattering (QENS) (including NSE) is much higher than that from macroscopic methods as dielectric spectroscopy, namely, about 0.45. Because QENS experiments are executed at higher temperature to place the relaxation into the observable window, the distribution of relaxation times is narrower. If QENS relaxation curves are (force) fitted by a Kohlrausch law the narrow distribution will result in a β exponent close to the elementary 1/2.

Since the shape and temperature dependences follow from the same model, the only additional free parameter in the fit of the NSE data is the ratio between the dielectric and NSE relaxation times (23) which is expected to be a function of the wave vector Q of the NSE experiment. Currently, not much is known about the microscopic origin of this "coupling factor" $R_{NSE/D}(Q)$. Although all previous studies on other polymers did not follow exactly the prescription used here [to fit the whole NSE relaxation with the same relaxation function $\Phi(t)$ as the dielectric spectra], from literature,[17–19] it can be summarized that at the structure factor peak $R_{NSE/D}(Q_{max})=0.2-2$ and for the first minimum of $S(Q)$ above Q_{max} it is about five times smaller. This difference is either attributed to the De Gennes[20] narrowing or to the different form factors of α and β relaxations, which may both contribute to $S(Q,t)/S(Q)$. The absolute values obtained here fall well into the literature range. Nevertheless, for pure PVC the difference of $R_{NSE/D}(Q)$, and thus $\tau(Q)$ itself, between the structure factor peak ($Q=1.2$ Å^{-1}) and $Q=1.5$ Å^{-1} is unexpectedly small, the ratio being only about 1.4.

In order to assess the validity of this result it is important

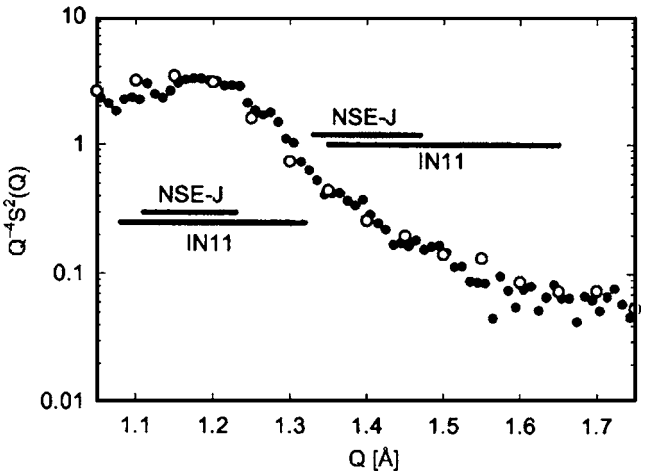

FIG. 16. Q dependence of coherent relaxation times expected from Sköld's formulation of the De Gennes narrowing for PVC (○) and PVC/DOP (●). The bars indicate the Q ranges over which IN11 (for PVC) and the Jülich NSE (for PVC/DOP) average.

to estimate the effect of the large wavelength spread of IN11. It can be expected that by averaging over the range $Q=1.2\pm0.12$ Å^{-1} NSE also picks up (lower) off-peak contributions in $\tau(Q)$. (This has been observed before on polyisobutylene which also has a rather sharp structure factor peak.[21]) There is no generally accepted quantitative relation between $S(Q)$ and $\tau(Q)$. But for an estimate it is sufficient to use Sköld's relation,[22]

$$S_{coh}(Q,t) = S(Q)S_{inc}\left(\frac{Q}{\sqrt{S(Q)}},t\right), \tag{24}$$

together with the Gaussian approximation of a Kohlrausch-type incoherent scattering function,

$$S_{inc}(Q,t) = \exp(-Q^2\tilde{D}t^\beta). \tag{25}$$

Inserting (25) into (24) and comparing with $S_{coh}(Q,t)/S(Q)=\exp(-(t/\tau_K)^\beta)$ yields

$$\tau_K(Q) \propto Q^{-2/\beta}S(Q)^{1/\beta}, \tag{26}$$

for $\beta=1/2$: $Q^{-4}S(Q)^2$. Note that if one just wants to estimate a ratio of relaxation times the distribution [Eq. (4)] does not play a role because all τ_K's are shifted by the same factor.

Figure 16 shows the De Gennes-Sköld factor $Q^{-4}S(Q)^2$ for PVC and PVC/DOP derived from diffraction data. $S(Q)$ data for PVC are from an experiment on the triple-axis spectrometer SV-4 in Jülich[12] and for PVC/DOP from the powder diffractometer SV-7.[13] Because both structure factors are very similar also the expected Q dependences of the relaxation times do not differ much. Table III shows the ratios $\tau_K(Q=1.2\text{ Å}^{-1})/\tau_K(Q=1.5\text{ Å}^{-1})$ for PVC [and $\tau_K(Q=1.17\text{ Å}^{-1})/\tau_K(Q=1.4\text{ Å}^{-1})$ for PVC/DOP] expected from the De Gennes narrowing in the Sköld formulation. The first row contains the values expected for ideally defined Q, while the second those taking into account the wavelength spread of the instruments (indicated by the bars in Fig. 16). One can see that the wavelength spread roughly halves the narrowing for PVC but does not reduce it to the factor of 1.4 observed

TABLE III. Ratios $\tau_K(Q=1.2\ \text{Å}^{-1})/\tau_K(Q=1.5\ \text{Å}^{-1})$ for PVC and $\tau_K(Q=1.17\ \text{Å}^{-1})/\tau_K(Q=1.4\ \text{Å}^{-1})$ for PVC/DOP expected from the Sköld/De Gennes picture compared to the experimental result. The first row refers to an ideal Q definition while the second takes the Q smearing due to different $\Delta\lambda/\lambda$ on IN11 and the Jülich NSE into account.

	PVC	PVC/DOP
Expected τ_K ratio	21	9.7
Expected considering $\Delta\lambda/\lambda$	12.5	9.5
Measured	1.4	6.7

here experimentally. Therefore, we conclude that the absence of the De Gennes narrowing in PVC is true and not due to instrumental effects.

Concerning the plasticization effect, at the structure factor peak NSE observes about the same acceleration of the dynamics as dielectric spectroscopy. This can be seen from the roughly agreeing values of $R_{NSE/D}(Q)$. In absolute terms of relaxation time, while at 390 K the dielectric relaxation becomes faster by a factor of 5.4 due to plasticization, the NSE relaxation time at $Q=1.2\ \text{Å}^{-1}$ changes by 679 ns/167 ns=4.1. This is the expected result (α relaxation universality) because at the structure factor peak NSE observes predominantly the α relaxation.

On the first glance it is then surprising that the plasticizer effect on the relaxation at 1.4–1.5 Å^{-1}, near the structure factor minimum, is much higher. Instead of 5.4 expected from dielectric spectroscopy we find a factor of about 20. But it is known that the behavior of the microscopic density fluctuation relaxation for Q above the structure factor peak does not follow that of the macroscopic α relaxation.[23] The reason is that at Q values off the structure factor peak other relaxation processes besides the α relaxation may dominate the decay of density correlations. This could in most cases be identified as the β relaxation.[11,24] This specific origin would not lead to a stronger plasticization here because the plasticizer effect on the β relaxation (Fig. 4) is even weaker than that on the α relaxation. Nevertheless, by the same argument fast relaxations in the plasticizer itself could become visible at off-peak Q values. Because these are trivially not present in pure PVC this would also explain the large effect of the plasticizer at high Q. This would also explain why the ratio of $\tau(Q)$ between the structure factor and 1.4 Å^{-1} is in the "normal" range for PVC/DOP, namely, about 7: The anomaly of pure PVC would be masked by the additional dynamical contribution of DOP.

From Table III one can see that due to the better wavelength definition of the Jülich NSE the instrumental distortion of the $\tau(Q)$ ratio is expected to be negligible. Also the expected ratio $\tau_K(Q=1.17\ \text{Å}^{-1})/\tau_K(Q=1.4\ \text{Å}^{-1})=9.5$ compares better with the experimental one.

V. CONCLUSIONS

We have performed a comparative study of a plasticized polymer (PVC/dioctylphthalate) and its pure counterpart (PVC) by dielectric spectroscopy and neutron spin echo (NSE) spectroscopy. Data from both methods could successfully be described by a model of the α relaxation using stretched exponentials with distributed relaxation times devised in Ref. 4. In contrast to that earlier work an asymmetric distribution function became necessary. The difference of the study reported here is that it goes to lower temperatures. There, the systems may fall out of equilibrium but also the separation of conductivity and α relaxation becomes more difficult. The α relaxation parameters width and skewness are at the *same characteristic relaxation time* identical for PVC and PVC/DOP. All differences of the plasticized and neat polymer compared at same temperatures can be traced back to the (VFT) temperature dependence of the α relaxation time changed by the plasticizer. In other words, the plasticizer only remaps the temperature scale. In contrast to this for the β relaxation the same width is found at *same temperatures* for PVC and PVC/DOP.

The fact that the same model holds for both PVC and PVC/DOP also shows that the relaxations of PVC and DOP are *coupled*. Although DOP has a dipole moment and therefore also contributes to the dielectric spectra it does not create a separate peak or even a change of the shape of the relaxation time distribution.

For the intermediate scattering function $S(Q,t)/S(Q)$ measured by NSE the slowing down of the α relaxation close to the structure factor peak is unexpectedly small for pure PVC, namely, only 1.4 between $Q=1.2\ \text{Å}^{-1}$ and $Q=1.5\ \text{Å}^{-1}$. This is true in comparison to the commonly found value of about 7 for other polymers as well as to the value expected from the De Gennes-Sköld picture in this particular system (12.5). For PVC/DOP this ratio is 6.7, comparable to the observation on other polymers and also roughly agreeing with the De Gennes-Sköld calculation (9.5).

APPENDIX: PROPERTIES OF THE GAMMA DISTRIBUTION

To cope with the dielectric loss function occurring here which shows strong high frequency tails on a logarithmic frequency scale we need an asymmetric distribution function for the Kohlrausch times. For this purpose we chose the *gamma distribution*,

$$g(\ln \tau_K) = \frac{b/\ln 10}{\Gamma(p)} x^{p-1} \exp(-x), \tag{A1}$$

of the rescaled logarithmic inverse normalized relaxation time,

$$x = b \log_{10}(\tau_{max}/\tau_K). \tag{A2}$$

The scaling time τ_{max} defines the maximum Kohlrausch time for which (A1) is defined. For $\tau_K \geqslant \tau_{max}$, $g(\ln \tau_K)=0$ is assumed. As Fig. 17 shows the high time cutoff at that value is rather sharp while there is an extended wing towards low times. This yields the asymmetry necessary to describe the experiments. The strength of this asymmetry is determined by the parameter $p>0$. Larger values of p result in a more symmetric shape. The factor b rescales the (logarithmic) width of the distribution. Without this factor the width would be also determined by p according to the original definition (A1) with $b=1$.

Alternatively, Eqs. (A1) and (A2) can be expressed as

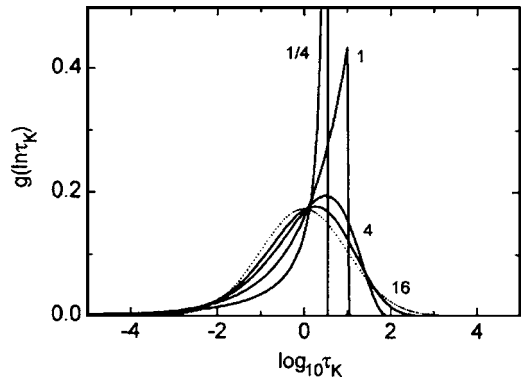

FIG. 17. Rescaled gamma distribution [Eqs. (A1) and (A2)] for $p=1/4$, 1, 4, and 16, i.e., skewnesses $\gamma_1=-2$, -1, $-1/2$, and $-1/4$. The parameters b and $\log_{10}\tau_{\max}$ are chosen accordingly so that $\langle\log_{10}\tau_K\rangle=0$ and $W=1$. The dotted line shows the log-normal distribution (A10) which is the limiting distribution for $p\to\infty$.

the *Pearson type III distribution*,[25,26]

$$g(\ln\tau_K)=\frac{1}{\beta\Gamma(p)}y^{p-1}\exp(-y)\quad\text{with } y=\frac{x-\alpha}{\beta}, \tag{A3}$$

with $x=\log_{10}\tau_K$, $\alpha=\log_{10}\tau_{\max}$, and $\beta=-1/b$.

Distribution (A1) is also a special case of a distribution called generalized exponential (GEX) distribution by Nicolai *et al.*[27] or generalized gamma (GG) distribution by Blochowicz *et al.*,[28] which are also applied for the description of relaxations in glass-forming systems. Nevertheless, there are two fundamental differences between their treatment and ours: (1) The argument of the distribution is proportional to τ in their papers while it is linear in $\log\tau$ in ours. So their function will approach a normal distribution of τ in case of vanishing skewness while ours approaches a log-normal distribution. (The latter was found in the earlier study[4] and of course this limit has to be reproduced here.) (2) While Nicolai *et al.* and Blochowicz *et al.* use GEX and GG as a distribution of *exponentials* we use it as distribution of *Kohlrausch functions*. So we use this distribution only for the extrinsic broadening due to the heterogeneity in PVC and PVC/DOP while they use it to describe the intrinsic broadening of the α relaxation.

For $p\geqslant 1$ the distribution (A1) has its maximum at $x=p-1$ corresponding to $\tau_K=10^{-p+1}\tau_{\max}$. For $p<1$ the distribution diverges for $x\to 0$. This may be used as an argument that parameters $p=0-1$ are not "physically reasonable." Nevertheless, since we cannot expect an empirical expression to describe the real distribution exactly we can still consider it as a valid approximation. We also point out that all moments of the distribution which will be calculated in the following are regular and continuous functions of p over the whole range $p=0$ to ∞.

The center of mass of the distribution on the logarithmic abscissa is

$$\langle\log_{10}\tau_K\rangle=\log_{10}\tau_{\max}-\frac{p}{b}. \tag{A4}$$

It has to be noted that this value is distinct from the logarithm of the average Kohlrausch time. The latter is

$$\langle\tau_K\rangle=\left(1+\frac{\ln 10}{b}\right)^{-p}\tau_{\max}. \tag{A5}$$

Only for high b, i.e., small width of the distribution, both averages can be reconciled because $\langle\log_{10}\tau_K\rangle=\log_{10}\langle\tau_K\rangle+O(1/b^2)$.

It is common to define the width W of a distribution of relaxation times as the standard deviation of the distribution on a (base 10) logarithmic abscissa.[29] With this definition we obtain

$$W^2=\langle(\log_{10}\tau_K-\langle\log_{10}\tau_K\rangle)^2\rangle=\frac{p}{b^2}. \tag{A6}$$

Similarly, the third centralized moment of the distribution $g(\ln\tau_K)$ is

$$\langle(\log_{10}\tau_K-\langle\log_{10}\tau_K\rangle)^3\rangle=-\frac{p}{b^3}. \tag{A7}$$

Here, the minus sign indicates that the distribution is skewed towards the left side. The common measure of "skewness" in the systematics of probability functions is obtained by dividing (A7) by the variance (A6) to the power 3/2:

$$\gamma_1=-\frac{1}{\sqrt{p}}. \tag{A8}$$

From this expression one can see that for $p\to\infty$ the skewness of the distribution vanishes. This implies that the distribution becomes symmetric for large p but not necessarily that it develops into a normal distribution. To show this, one has to calculate the limit of $g(\log_{10}\tau_K)$ for $p\to\infty$ keeping the width W and center $\langle\log_{10}\tau_K\rangle$ constant. This can be done by using the characteristic function of (A3):[26]

$$\phi(t)=e^{i\alpha t}(1-i\beta t)^{-p}. \tag{A9}$$

We substitute α and β by the given values of W and $\langle\log_{10}\tau_K\rangle$ and apply de Moivre's theorem:

$$\phi(t)=e^{i(\langle\log_{10}\tau_K\rangle+W\sqrt{p})t}\left(1+\frac{W^2}{p}t^2\right)^{-p/2}e^{-ip\arctan(W/\sqrt{p}t)}.$$

If we now take the limit $p\to\infty$ the middle term is just Euler's limit with the argument $-W^2t^2/2$. The arctangent can be linearized in this limit and the resulting term cancels the $-iW\sqrt{p}t$ in the first exponential leaving finally

$$\lim_{p\to\infty}\phi(t)=e^{i\langle\log_{10}\tau_K\rangle t+W^2t^2/2},$$

which is immediately recognizable as the characteristic function of the normal distribution,

$$g_{p\to\infty}(x)=\frac{1}{\sqrt{2\pi}W}e^{-(1/2)((x-\langle\log_{10}\tau_K\rangle)/W)^2}, \tag{A10}$$

with $x=\log_{10}\tau_K$.

The calculation of the integral (4) with the distribution (A1) inserted causes considerable numerical difficulties. If p increases—which will happen if the data require a description by a more symmetric function—the gamma function yields excessive values. For large p, it is therefore necessary to calculate the logarithm of the whole expression (A1) first

using Stirling's formula for $\ln \Gamma(p)$. For even larger p, the limit (A10) can be used as soon as it is numerically indistinguishable from the exact value.

[1] R. L. Scherrenberg, H. Reynaers, C. Gondard, and J. P. Verluyten, Macromolecules **26**, 4118 (1993).
[2] W. Barenswaard, V. Litvinov, F. Souren, R. Scherrenberg, C. Gondard, and C. Colemonts, Macromolecules **32**, 167 (1999).
[3] See, for example, N. G. McCrum, B. E. Read, and G. Williams, *Anelastic and Dielectric Effects in Polymeric Solids* (Dover, New York, 1991), p. 422, and references therein.
[4] A. Arbe, A. Moral, A. Alegría, J. Colmenero, W. Pyckhout-Hintzen, D. Richter, B. Farago, and B. Frick, J. Chem. Phys. **117**, 1336 (2002).
[5] F. Alvarez, A. Alegría, and J. Colmenero, Phys. Rev. B **44**, 7306 (1991).
[6] F. Alvarez, A. Alegría, and J. Colmenero, Phys. Rev. B **47**, 125 (1993).
[7] P. Lunkenheimer and A. Loidl, Chem. Phys. **284**, 205 (2002).
[8] R. Zorn, A. Alegría, A. Arbe, J. Colmenero, D. Richter, and B. Frick, J. Non-Cryst. Solids **235–237**, 169 (1998).
[9] J. J. del Val, A. Alegría, J. Colmenero, and C. Lacabanne, J. Appl. Phys. **59**, 3829 (1986).
[10] S. Savranski (private communication).
[11] A. Arbe, D. Richter, J. Colmenero, and B. Farago, Phys. Rev. E **54**, 3853 (1996).
[12] J. Colmenero, A. Arbe, G. Coddens, B. Frick, C. Mijangos, and H. Reinecke, Phys. Rev. Lett. **78**, 1928 (1997).
[13] R. Zorn and J. Walter, Experimental Report No. SV7-04-019 (Forschungszentrum Jülich, Jülich, 2004), http://www.fz-juelich.de/iff/pics_pdfs/wns/ER2004_SV7.pdf, p. 37.
[14] C. A. Angell, in *Relaxations in Complex Systems*, edited by K. L. Ngai and G. B. Wright (National Technical Information Service, Springfield, VA, 1984), p. 3.
[15] R. Böhmer, K. L. Ngai, C. A. Angell, and D. J. Plazek, J. Chem. Phys. **99**, 4201 (1993).
[16] W. Götze, in *Aspects of Structural Glass Transition*, edited by D. Levesque, J. Zinn-Justin, and J.-P. Hansen (North-Holland, Amsterdam, 1991), p. 289.
[17] D. Richter, B. Frick, and B. Farago, Phys. Rev. Lett. **61**, 2465 (1988).
[18] D. Richter, M. Monkenbusch, A. Arbe, J. Colmenero, B. Farago, and R. Faust, J. Phys.: Condens. Matter **11**, A297 (1999).
[19] R. Zorn, D. Richter, B. Farago, B. Frick, F. Kremer, U. Kirst, and L. J. Fetters, Physica B **180&181**, 534 (1992).
[20] P. G. De Gennes, Physica (Amsterdam) **25**, 825 (1959).
[21] D. Richter, A. Arbe, J. Colmenero, M. Monkenbusch, B. Farago, and R. Faust, Macromolecules **31**, 1133 (1998).
[22] K. Sköld, Phys. Rev. Lett. **19**, 1023 (1967).
[23] D. Richter, R. Zorn, B. Farago, B. Frick, and L. J. Fetters, Phys. Rev. Lett. **68**, 71 (1992).
[24] D. Richter, M. Monkenbusch, A. Arbe, J. Colmenero, and B. Farago, Physica B **241–243**, 1005 (1998).
[25] K. Pearson, Philos. Trans. R. Soc. London, Ser. A **186**, 343 (1895).
[26] M. Abramowitz and I. A. Stegun, *Handbook of Mathematical Functions* (Dover, New York, 1970).
[27] T. Nicolai, J. Ch. Gimel, and R. Johnsen, J. Phys. II (France) **6**, 697 (1996).
[28] Th. Blochowicz, Ch. Tschirwitz, St. Benkhof, and E. A. Rössler, J. Chem. Phys. **118**, 7544 (2003).
[29] This tradition seems to go back to the description of the β relaxation by Wu and Nagel [L. Wu and S. R. Nagel, Phys. Rev. B **46**, 11198 (1992)] as the normal distribution of base 10 logarithms of the logarithms of the frequencies. Although in this way formulas are complicated by the unexpected occurrence of ln 10 factors, we will stick to the convention.